Distinct roles for two *C. elegans* anillins in the gonad and early embryo

Amy Shaub Maddox[1,*], Bianca Habermann[2], Arshad Desai[1] and Karen Oegema[1,*]

[1]Ludwig Institute for Cancer Research, Department of Cellular and Molecular Medicine, University of California, San Diego, 9500 Gilman Drive, La Jolla, CA 92093, USA
[2]Scionics Computer Innovation, Pfotenhauerstrasse 110, Dresden 01307, Germany
*Authors for correspondence (e-mail: amaddox@ucsd.edu; koegema@ucsd.edu)

Accepted 18 March 2005

Development 132, 2837-2848
Published by The Company of Biologists 2005
doi:10.1242/dev.01828

Summary

Anillins are conserved proteins that are important for stabilizing and remodeling the actin cytoskeleton. Anillins have been implicated in cytokinesis in several systems and in cellularization of the syncytial *Drosophila* embryo. Here, we examine the functions of three *C. elegans* proteins with homology to anillin (ANI-1, ANI-2 and ANI-3). We show that ANI-1 and ANI-2 contribute to embryonic viability by performing distinct functions in the early embryo and gonad, respectively. By contrast, ANI-3 appears to be dispensable for embryonic development. ANI-1 is essential for cortical ruffling and pseudocleavage, contractile events that occur in embryos prior to mitosis. ANI-1 is also required for the highly asymmetric cytokinetic events that extrude the two polar bodies during oocyte meiosis, but is dispensable for cytokinesis following mitotic chromosome segregation. During both meiosis and mitosis, ANI-1 targets the septins, but not myosin II, to the contractile ring and does not require either for its own targeting. In contrast to ANI-1, ANI-2 functions during oogenesis to maintain the structure of the rachis, the central core of cytoplasm that connects the developing oocytes in the syncytial gonad. In ANI-2-depleted worms, oocytes disconnect prematurely from the defective rachis, generating embryos of varying sizes. Our results highlight specialization of divergent anillin family proteins in the *C. elegans* life cycle and reveal conserved roles for this protein family in organizing syncytial structures and cortical contractility.

Key words: Cytokinesis, Cellularization, Polarity, Cortical flows, Contractility

Introduction

Anillins are widely conserved proteins that have been implicated in cytokinesis and cellularization. Anillins are modular proteins that are thought to crosslink cytoskeletal components at the cell cortex by interacting directly with both filamentous actin (F-actin) and myosin II. The founding member of the anillin family, *Drosophila* anillin, was identified based on its ability to bind and bundle actin filaments (Field and Alberts, 1995), and actin-binding domains have been defined in the N termini of *Drosophila, Xenopus* and human anillins (Field and Alberts, 1995; Kinoshita et al., 2002; Oegema et al., 2000). A domain of *Xenopus* anillin that binds directly to phosphorylated non-muscle myosin II has also been defined (Straight et al., 2005).

A characteristic sequence feature of all anillin family members is a C-terminal pleckstrin homology (PH) domain. The PH domains of human anillin and the *S. pombe* anillin-related protein Mid2 are required for targeting to the contractile ring (Berlin et al., 2003; Oegema et al., 2000; Tasto et al., 2003). The PH domain may mediate interactions with plasma membrane lipids and/or with cortical proteins such as the septins (Kinoshita et al., 2002; Oegema et al., 2000; Field et al., 2005). Septins are conserved guanine nucleotide-binding proteins that are thought to be components of a membrane-associated cytoskeletal filament system (Kinoshita, 2003). Isolated septin filaments associate specifically with actin bundled by human anillin, but not by other actin-binding proteins (Kinoshita et al., 2002). The interaction between anillin and the septins defined in vitro is supported by similar cellularization and cytokinesis defects observed in septin and anillin mutant *Drosophila* embryos (Adam et al., 2000; Neufeld and Rubin, 1994; Field et al., 2005). Similarly, *S. pombe* cells deleted for Mid2 or null for septin function exhibit an identical non-lethal delay in septation (Berlin et al., 2003; Longtine et al., 1996; Tasto et al., 2003).

Anillins have primarily been implicated in cortical remodeling during cytokinesis and cellularization. In *Drosophila* and human cells in which anillin is inhibited by RNAi (Echard et al., 2004; Eggert et al., 2004; Kiger et al., 2003; Rogers et al., 2003; Somma et al., 2002; Straight et al., 2005) or mutation (Field et al., 2005), contractile rings form and ingress, but cytokinesis fails to complete. Cytokinesis failure is accompanied by cortical blebbing surrounding the bridge that connects the two daughter cells, suggesting that anillin acts late in cytokinesis to facilitate completion (Echard et al., 2004; Somma et al., 2002; Straight et al., 2005). Although neither of the two anillin-related proteins in *S. pombe* is essential, both contribute to cytokinesis. Mid1 is the first protein recruited to the medial ring and is required for its proper placement (Bahler et al., 1998; Sohrmann et al., 1996;

Wu et al., 2003). Mid2 acts later to stabilize septin localization and facilitate cell separation (Berlin et al., 2003; Tasto et al., 2003). In addition to its role in cytokinesis, *Drosophila* anillin also has a crucial role during cellularization of the syncytial embryo (Field et al., 2005). Cellularization occurs when the ~6000 nuclei created during the first 13 synchronous nuclear divisions are simultaneously partitioned by membranes deposited behind furrows that ingress inwards from the embryo surface (Mazumdar and Mazumdar, 2002; Miller and Kiehart, 1995).

Embryos of the nematode *C. elegans* exhibit stereotypical cortical contractile events, including polar body extrusion, cortical ruffling, pseudocleavage and cytokinesis (Wood, 1988). In addition, oogenesis in *C. elegans* is a gradual cellularization event that involves extensive cortical remodeling in a syncytial gonad that bears some resemblance to the cellularizing *Drosophila* embryo (Hubbard and Greenstein, 2000). We describe the functional characterization of three *C. elegans* anillin homologs, ANI-1, ANI-2 and ANI-3. We show that ANI-2 functions specifically in the syncytial gonad, where it is required to maintain gonad structure and promote proper oogenesis. By contrast, ANI-1 modulates cortical contractility in the early embryo and also functions later in development. ANI-1 is required to concentrate myosin II into cortical patches to generate productive ingressions during ruffling and pseudocleavage, which normally occur concurrent with the establishment of polarity in the one-cell stage embryo (Cowan and Hyman, 2004). ANI-1 is also required to target the septins, but not myosin II, to contractile rings during polar body formation and cytokinesis. Interestingly, polar body extrusion fails in ANI-1-depleted embryos, but ingression of the cleavage furrow during cytokinesis appears to occur normally. Our results highlight both the conserved functions of the anillin protein family, and the adaptations that enable it to meet the specific requirements of the *C. elegans* life cycle.

Materials and methods

Worm strains

Strains expressing NMY-2:GFP and PAR-6:GFP (Nance et al., 2003) were a kind gift of Edwin Munro. *rde-1(ne300)* was provided by Amy Pasquinelli. CB228 carrying the e228 *unc-61* truncation allele (Nguyen et al., 2000) was provided by the CGC (see Table S1 in the supplementary material).

RNA-mediated interference

dsRNA was prepared as described (Oegema et al., 2001). DNA templates were prepared using primers (see Table S2 in the supplementary material) to amplify regions of N2 genomic DNA, N2 cDNA or specific cDNAs, as indicated. L4-stage hermaphrodites were injected with dsRNA and incubated at 20°C for 45-48 hours. Soaking RNAi was performed as described (Maeda et al., 2001), except worms were incubated in a drop of RNA solution on parafilm in a humid chamber for 24 hours at 20°C. Worms were then recovered to a seeded NGM (nematode growth medium) plate and incubated for 48 hours at 20°C.

Embryonic lethality and Brood size tests

RNAi-treated worms were placed on individual plates 48 hours after injection or 72 hours after soaking was initiated. After 24 hours at 20°C, the worms were removed from each plate and embryos and young larvae were grouped together and counted (average=brood size). Embryo viability was evaluated 24 hours or more later; unhatched eggs were counted and calculated as a percentage of total laid for that plate (embryonic lethality).

Microscopy

Immunofluorescence images were acquired and processed as described (Cheeseman et al., 2004). For live imaging, newly fertilized embryos were mounted as described (Oegema et al., 2001). DIC imaging was performed as described (Gonczy et al., 1999). For embryos expressing NMY-2:GFP, three *z*-sections were acquired at 1 μm intervals near the embryo surface using a spinning disc confocal equipped with a 60×, 1.40 NA Nikon PlanApo objective and 2×2 binning. Images were collected at 10 second intervals and the three images for each time point were projected for presentation.

Immunofluorescence and immunoblotting

Immunofluorescence was performed as described previously (Desai et al., 2003; Oegema et al., 2001). Polyclonal antibodies against ANI-1 (residues 460-768), ANI-2 (residues 890-1015), NMY-2 (residues 945-1368), UNC-59 (C-terminal peptide: (C)SGTMKKR-MGGLGLFNRN), UNC-61 [C-terminal peptide: (C)TEERMKL-MTKVSKKLRK] were generated as described previously (Desai et al., 2003). For fixation of gonads, adult worms in 5% sucrose, 100 mM NaCl were nicked with a scalpel to extrude the gonads. Western blotting of extracts prepared from embryos and adult hermaphrodites was performed using standard protocols and blotting of RNAi-depleted and control worms was performed as described (Hannak et al., 2001). To control for protein loading, blots were re-probed with antibodies to α-tubulin (DM1-α; Abcam).

Dextran injections

Dextran (70 kDa) labeled with tetramethylrhodamine (Molecular Probes) was reconstituted to 1 mg/ml in injection buffer (1 mM potassium citrate, 6.7 mM KPO_4, pH 7.5, 0.67% PEG) and injected into the gonad rachis of adult worms. After 5-15 minutes, worms were mounted whole in M9 buffer (22 mM KH_2PO_4, 19 mM NH_4Cl, 48 mM Na_2HPO_4, 9 mM NaCl) on multiwell glass slides. DIC and wide-field fluorescent images were acquired using a 20× 0.75 NA Nikon PlanApo objective, and 2×2 binning.

Results

The *C. elegans* genome contains three genes with homology to anillin

Sequence analysis revealed three *C. elegans* genes that encode proteins with similarity to anillins. Based on this homology, we named these genes *ani-1* (Y49E10.19), *ani-2* (K10B2.5) and *ani-3* (Y43F8C.14). cDNAs corresponding to all three genes have been isolated (www.wormbase.org, release WS133), indicating that they are all expressed. The highest level of sequence conservation among the *C. elegans* proteins and the anillins of other species is in the C-terminal pleckstrin homology (PH domain; grey in Fig. 1A) and the preceding ~280 amino acids, which we refer to as the 'Anillin Homology' (AH) domain (pink in Fig. 1A). Of the three *C. elegans* anillin family proteins, ANI-1 has the most extensive sequence conservation with the *Drosophila* and human proteins (Fig. 1A; see Fig. S1 in the supplementary material). Sequence comparisons revealed regions of ANI-1 with homology to the myosin II and actin-binding regions that have been defined for the human and *Drosophila* anillins. Regions with a similar level of homology were not identified in ANI-2 or ANI-3, suggesting that these domains are either not present or are highly divergent in these two proteins.

ANI-1 and ANI-2 have distinct roles in embryo production and viability

The divergence in the protein sequences of the three *C. elegans* anillin homologs suggests that they perform different functions. To determine whether the *C. elegans* anillins are required for embryo production or viability, we depleted each individually by RNAi using either injection or soaking. We then measured the number of embryos laid by the treated worms (brood size) and their viability. Consistent with the results of a large-scale screen (Kamath et al., 2003), RNAi of ANI-3 by either method had no effect on either brood size or embryonic viability (Fig. 1B,C). RNAi of ANI-3 also did not enhance any of the phenotypes resulting from depletion of ANI-1 or ANI-2 (discussed in detail below). Therefore, we did not characterize ANI-3 further.

Consistent with the results of previous screens (Gonczy et al., 2000; Kamath et al., 2003; Piano et al., 2000; Simmer et al., 2003), the number of embryos laid by *ani-1(RNAi)* worms was similar to controls (Fig. 1B), but highly penetrant embryonic lethality was observed (Fig. 1C). Quantitative western blotting using affinity-purified antibodies revealed that ANI-1 levels were reduced to ~3% of control by injection RNAi (Fig. 1D). Soaking also resulted in increased embryonic lethality but with lower penetrance. Consequently, for all subsequent experiments, injection of dsRNA was used to deplete ANI-1.

For ANI-2, soaking worms in dsRNA resulted in more severe phenotypes than injection. Soaking reduced the amount of ANI-2 to ~3% of control levels (Fig. 1D) and significantly reduced both the number of embryos laid by the treated worms and embryo viability (Fig. 1B,C). Similar effects on embryo production and viability have been reported previously (Kamath et al., 2003; Maeda et al., 2001). In contrast to our results for ANI-1, penetrant depletion of ANI-2 resulted in only a partial reduction of embryonic viability. Quantitative western blotting indicated that depletion of ANI-1 did not affect levels of ANI-2 and vice versa (Fig. 1D), confirming the specificity of the RNAi-mediated depletions and of the affinity-purified antibodies used to monitor ANI-1 and ANI-2.

The different consequences of depleting ANI-1 or ANI-2 on embryo production and viability suggest that these related proteins have distinct functions. Indeed, western blotting of extracts prepared from whole worms or isolated embryos revealed that ANI-1 is selectively enriched in embryos relative to adult hermaphrodites, whereas ANI-2 is highly enriched in adults relative to embryos (Fig. 1E). Immunofluorescence analysis of fixed embryos further underscored this difference. ANI-1 was detected on the cortex and localized prominently to the cytokinetic furrow of telophase embryos, whereas antibodies to ANI-2 did not recognize specific structures in embryos (Fig. 1F). From these results, we conclude that ANI-

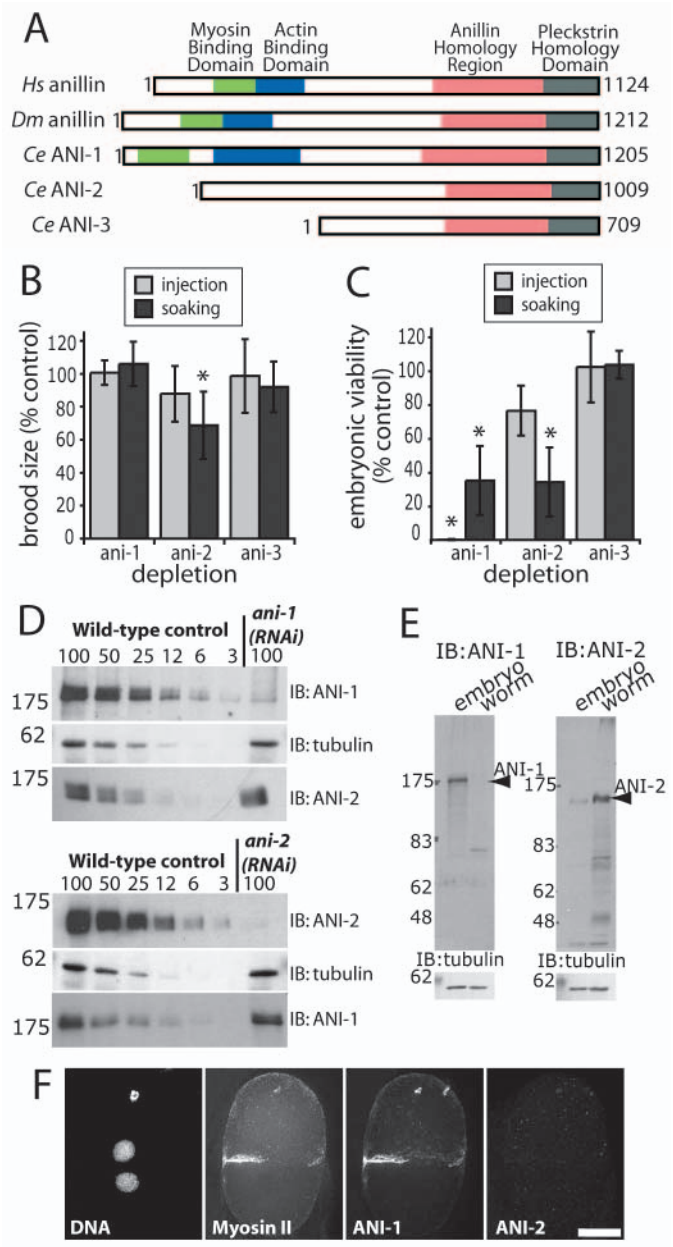

Fig. 1. *C. elegans* anillin-related proteins. (A) Schematics comparing features of the human and *Drosophila* anillins with the three *C. elegans* anillin homologs: C-terminal PH domains (grey); anillin homology (AH) regions (red); actin-binding and -bundling domains (blue); myosin-binding domains (green). For sequence comparisons, see Fig. S1B,C in the supplementary material. Worms were injected or soaked with dsRNA that targeted each of the anillin homologs. Embryos laid by the treated hermaphrodites between 48 and 72 hours after injection, or between 72 and 96 hours after the start of soaking, were counted (brood size, B) and the viability of the embryos (C) was measured. Data were normalized to the number and viability of embryos laid by worms treated with a control RNA against a yeast sequence not present in the *C. elegans* genome. Asterisks: significantly different from control ($P<0.05$, *t*-test; n=4-7 worms; ~100 embryos/worm). (D) Extracts from worms injected with *ani-1* dsRNA or soaked in *ani-2* dsRNA were analyzed by western blotting. Numbers above control lanes indicate percentage of amount loaded in 100% lane. The same blots were probed for α-tubulin as a loading control. (E) ANI-1 and ANI-2 are enriched in embryos and adult worms, respectively. Arrowheads indicate presumptive ANI-1 and ANI-2 bands. High-speed supernatants prepared from extracts of isolated embryos or whole worms were western blotted and probed with antibodies to ANI-1 and ANI-2. Blots were probed for α-tubulin as a loading control. Identical results were obtained with crude extract (data not shown). (F) A *C. elegans* embryo undergoing cytokinesis was fixed and stained with Hoechst to label DNA and specific antibodies to myosin II (NMY-2), ANI-1 and ANI-2. Scale bar: 10 μm.

1 is enriched in embryos and is required for their viability. By contrast, ANI-2, which contributes to both embryo production and viability, is primarily present in adult worms.

Polar body extrusion, ruffling and pseudocleavage fail in *ani-1(RNAi)* embryos, but cytokinesis occurs normally

The penetrant embryonic lethality resulting from depletion of ANI-1 suggested a role in embryonic development. To characterize the function of ANI-1, we analyzed cortical dynamics between fertilization and the first embryonic cytokinesis using DIC microscopy (Fig. 2; see Movies 1 and 2 in the supplementary material). In control wild-type embryos, immediately following fertilization the oocyte-derived nucleus undergoes two rounds of meiotic division, each of which ends with a small asymmetric cytokinesis-like event that extrudes a polar body. During the meiotic divisions, membrane ruffling occurs over the entire embryo surface. As embryonic polarity is established, ruffling becomes limited to the embryo anterior (Fig. 2A) (Cowan and Hyman, 2004). The oocyte pronucleus subsequently migrates towards the sperm pronucleus and the cortical ruffles resolve to form a transient invagination called the pseudocleavage furrow (Fig. 2B) that regresses as the pronuclei meet. Following nuclear envelope breakdown, spindle assembly and chromosome segregation, a cytokinetic furrow ingresses between the separated chromosome masses to generate the two daughter cells (Fig. 2E).

In ANI-1-depleted embryos, defects were observed in all of the early contractile events. Polar body extrusion was either abnormal, leading to the formation of a large bleb containing yolk granules and cytoplasm (Fig. 2A′, arrowhead), or failed completely, allowing the polar body chromatin to reenter the embryo (Fig. 2B′,E′, arrow). Cortical ruffles and the pseudocleavage furrow also failed to form following ANI-1 depletion (Fig. 2A′,B′). However, in surprising contrast to the complete failure of early contractile events, the positioning and ingression of the cytokinetic furrow appeared normal (Fig. 2D′). Cytokinesis also completed successfully and the cell-cell boundary remained intact beyond the four-cell stage in all ANI-1-depleted embryos (n=20). Simultaneous depletion of either ANI-2 or ANI-3 with ANI-1 did not exacerbate any of the defects observed in the ANI-1-depleted embryos (data not shown), suggesting that they do not function redundantly with ANI-1 in the early embryo. Thus, ANI-1 is required for early contractile events, including polar body formation, ruffling and pseudocleavage, but appears to be dispensable for cytokinesis.

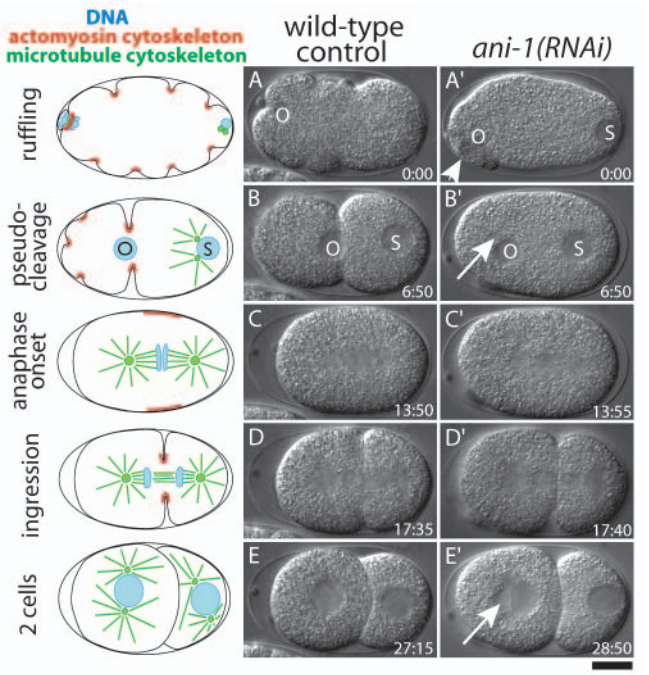

Fig. 2. Polar body extrusion, ruffling and pseudocleavage fail in *ani-1(RNAi)* embryos, but cytokinesis appears normal. Schematic drawings of *C. elegans* early embryonic development (left column) and selected images from timelapse DIC sequences of control (A-E) and *ani-1(RNAi)* (A′-E′) embryos. Embryo anterior is on the left; posterior (defined by the site of sperm entry) is on the right. Arrow indicates a polar body nucleus that has entered the embryo. Scale bar: 10 μm.

ANI-1 is required to target the septins, but not myosin II, to contractile rings

ANI-1 is required for polar body extrusion, but not cytokinesis. Assembly of acto-myosin rings accompanies both events. To analyze the role of ANI-1 in greater detail, we examined the targeting of non-muscle myosin II (NMY-2) (Guo and Kemphues, 1996) and the two *C. elegans* septins (UNC-59 and UNC-61) (Nguyen et al., 2000) to meiotic and mitotic contractile rings in *ani-1(RNAi)* embryos. Consistent with their successful ingression, ANI-1 depleted telophase embryos possessed equatorial contractile rings enriched for NMY-2 (Fig. 3A,B). ANI-1 depletion also did not prevent NMY-2 from targeting to the small cortical rings that formed around the site of polar body extrusion (Fig. 3D). Interestingly, however, the septins, UNC-59 (Fig. 3) and UNC-61 (data not shown), failed to enrich in both the mitotic (Fig. 3A,B) and meiotic (Fig. 3D) cytokinetic rings in ANI-1-depleted embryos. During the first mitosis, the septins are normally on the anterior cortex and become highly enriched in the contractile ring at the leading edge of the ingressing furrow (red arrowheads in Fig. 3A,B). In *ani-1(RNAi)* embryos, the septins localized properly to the anterior cortex (Fig. 3A) but failed to concentrate at the cell equator preceding contractile ring ingression (data not shown) and were not enriched at the tip of the ingressing furrow compared with the adjacent cell-cell boundary (Fig. 3A,B, red arrowheads versus arrows). From these results, we conclude that ANI-1 is required to target the septins, but not myosin II, to contractile rings during both meiosis and mitosis.

ANI-1 targets independently of the septins and myosin II during mitosis and meiosis

To determine whether ANI-1 and the septins are interdependent for their localization, we analyzed septin-depleted embryos using worms homozygous for an *unc-61* mutant allele (*e228*) (Nguyen et al., 2000), or embryos depleted of UNC-59 and UNC-61 by double RNAi. Both ANI-1 and NMY-2 targeted to contractile rings during cytokinesis (Fig. 3A) and polar body formation (Fig. 3D) in septin loss-of-function embryos (only *unc-61* embryos are shown). The targeting of NMY-2 is consistent with the fact that that cytokinesis and polar body formation are successful in both types of septin loss-of-function embryos (Nguyen et al., 2000).

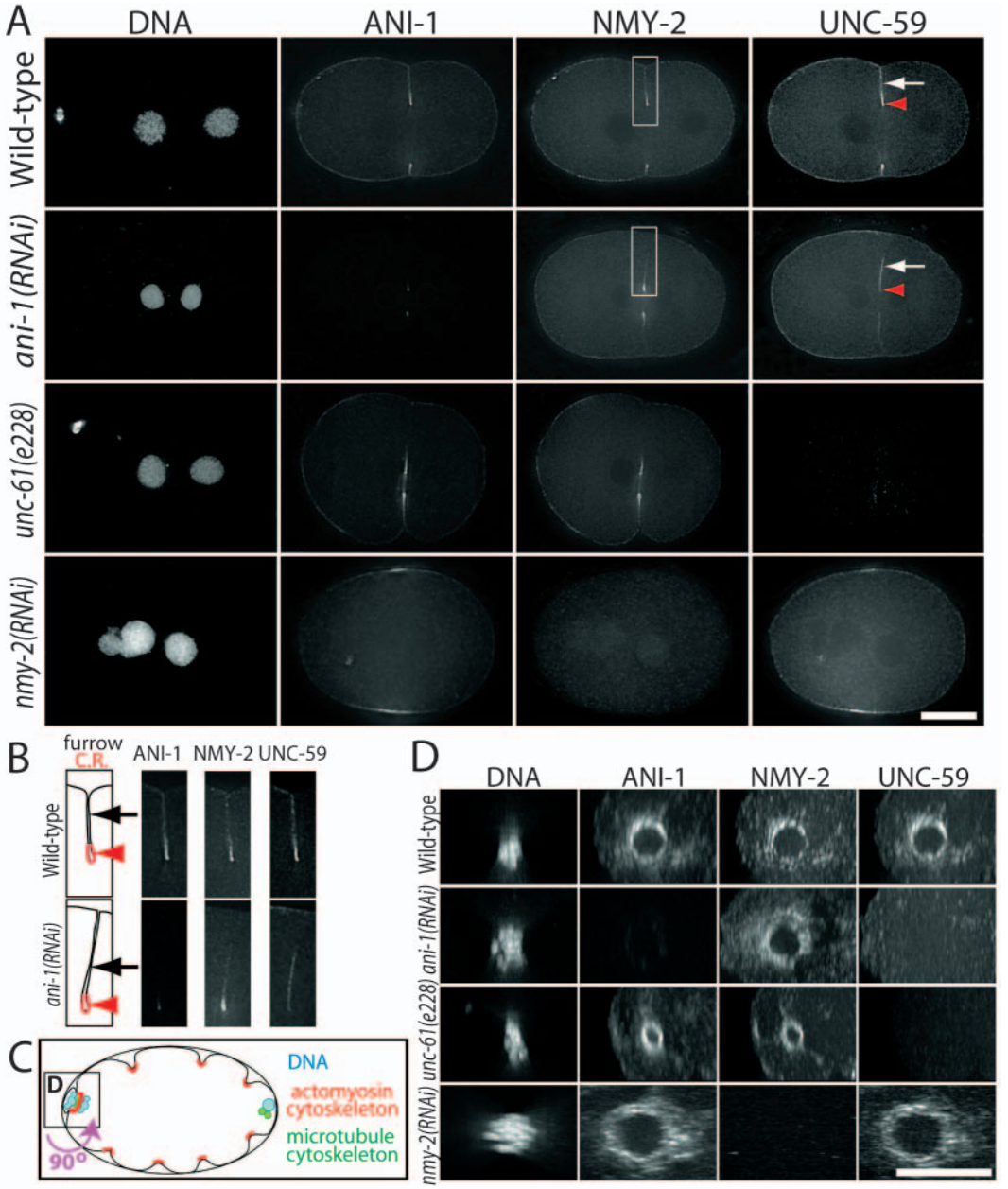

Fig. 3. (A) ANI-1 is required to target the septins, but not myosin II to the contractile ring. Control, *ani-1(RNAi)*, *unc-61(e228)* and *nmy-2(RNAi)* telophase embryos were fixed and stained for DNA, ANI-1, myosin II (NMY-2) and the septin UNC-59. Images are equivalently scaled. Only very low amounts of residual ANI-1 are detected in *ani-1(RNAi)* embryos. The contractile ring at the tip of the ingressing furrow (red arrowheads) and the new cell-cell boundary, which forms behind the ingressing furrow and consists of two juxtaposed cortical surfaces (white arrows), are indicated. The furrow does not ingress in *nmy-2(RNAi)* embryos. Scale bar: 10 µm. (B) Insets from the images in A are magnified twofold. The new cell-cell boundary (black arrows) and contractile ring (C.R., red arrowheads) are indicated. (C) Schematic showing location and orientation of magnified view in D. (D) Embryos undergoing polar body extrusion were fixed and stained for ANI-1, NMY-2 and UNC-59. In control embryos, all three proteins localize to a ring around the site of polar body extrusion. Images have been rotated so that this ring is viewed end on. Scale bar: 10 µm.

Cumulatively, our targeting analysis places ANI-1 upstream of the septins in contractile ring assembly.

We also examined *nmy-2(RNAi)* embryos to determine if NMY-2, or contractility, is required for ANI-1 localization. Despite the failure of ingression in *nmy-2(RNAi)* embryos, both ANI-1 and the septins accumulated in an equatorial band in telophase embryos (Fig. 3A), and at sites of attempted polar body formation (Fig. 3D). Thus, ANI-1 and the septins can be recruited to cytokinetic rings independently of NMY-2. Cumulatively, we conclude that similar dependency relationships exist during the assembly of the mitotic contractile ring and the smaller cortical rings that form around the site of polar body extrusion during meiosis. In both cases, ANI-1 is required to target the septins, but not myosin II, to the division site. In addition, targeting of ANI-1 does not require either myosin II or the septins.

ANI-1 organizes myosin II and the septins into cortical patches to promote ruffling

In contrast to cytokinesis, ruffling and pseudocleavage fail in ANI-1-depleted embryos (Fig. 2). To characterize these defects further, we examined the localization of NMY-2 and the septins in embryos fixed at times between the completion of meiosis II and pronuclear migration, when ruffling and pseudocleavage normally occur. During this period in control embryos, ANI-1, the septins and NMY-2 all concentrate in cortical patches (Fig. 4A,C). Although membrane invaginations are not preserved by the fixation used here, timelapse imaging of embryos expressing NMY-2:GFP (see Fig. 5B), GFP:UNC-59 or GFP:ANI-1 (data not shown) indicates that these patches correspond to the base of ingressing ruffles.

In ANI-1-depleted embryos, distinct cortical patches containing NMY-2 and the septins fail to form. Instead, both

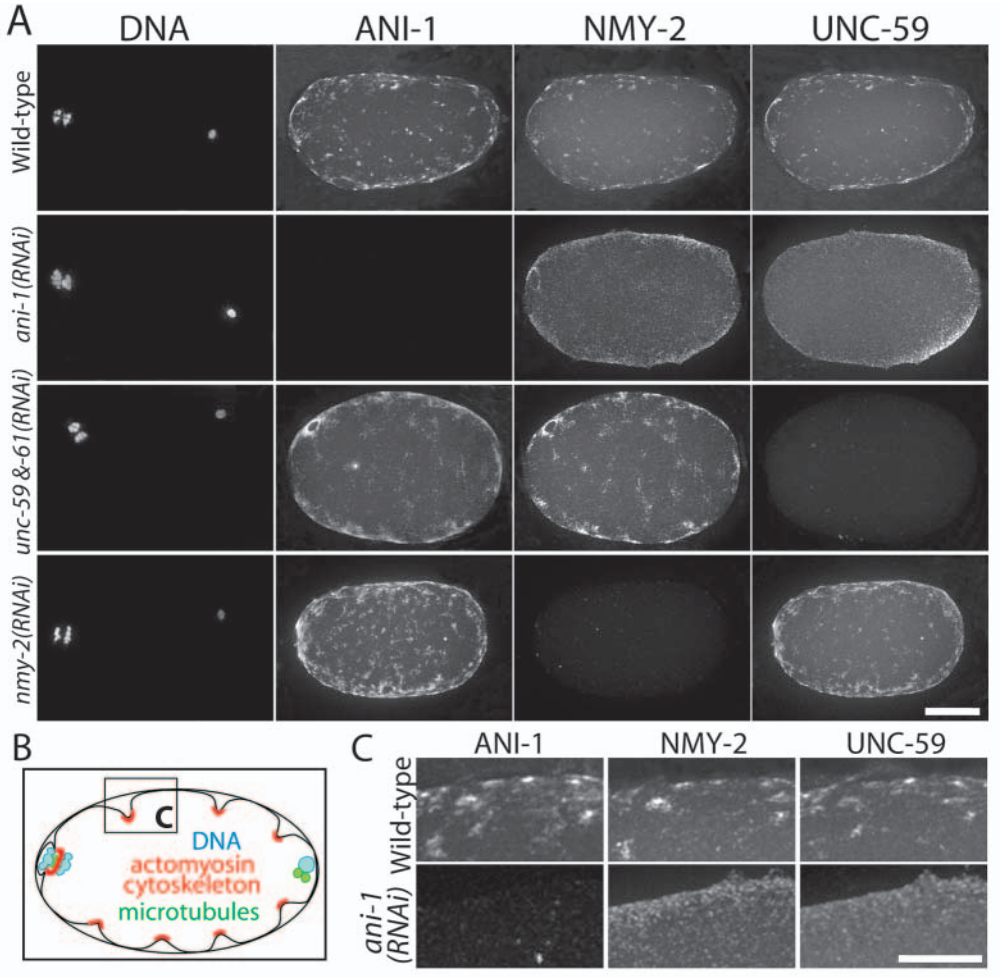

Fig. 4. ANI-1 is required for the formation of cortical patches containing myosin II and the septins. (A) Wild-type embryos and embryos depleted of ANI-1, both UNC-59 and UNC-61, or NMY-2 were fixed prior to pronuclear migration (when the anterior cortex normally ruffles) and stained for ANI-1, NMY-2 and UNC-59. Ruffles are not preserved by the fixation. In wild-type embryos, all three proteins concentrate in an inhomogeneous network of cortical patches. In *ani-1(RNAi)* embryos, UNC-59 and NMY-2 are diffuse on the cortex. Scale bar: 10 μm. (B) Schematic showing region of embryo magnified in C. (C) Magnified view of the cortex from control and *ani-1(RNAi)* embryos in A. Scale bar: 5 μm.

remain homogeneous at the cortex (Fig. 4A,C; results for UNC-61 not shown). A similar defect in the organization of the cortical cytoskeleton was observed in living ANI-1-depleted embryos expressing NMY-2:GFP (see Fig. 5B) or GFP:UNC-59 (data not shown). Interestingly, distinct patches of ANI-1 and the septins formed in embryos in which NMY-2 was depleted below the level of detection by immunofluorescence (Fig. 4A). NMY-2 depleted embryos failed to ruffle, further indicating that neither NMY-2 protein nor contractility is required for the organization of ANI-1 and the septins (and presumably other components of the cortical cytoskeleton) (Munro et al., 2004) into an inhomogeneous network. We conclude that ANI-1 promotes ruffling via a crucial role in organizing the cortical cytoskeleton to form inhomogeneities that become contractile in the presence of NMY-2 (see Fig. 9).

Perturbation of NMY-2 organization by depletion of ANI-1 does not prevent polarity establishment

Recent studies have suggested that a dynamic acto-myosin network generates an anterior-directed flow of NMY-2 and other cortical components that is important for polarity establishment (Cheeks et al., 2004; Munro et al., 2004). To determine whether flows occur normally in the absence of ANI-1, we analyzed the movement of yolk granules using kymographs generated from timelapse DIC sequences. Moving yolk granules present in successive frames appear as diagonal lines in the kymographs. Although there is considerable variability in the rate of movement of individual granules in both conditions, patterns of cortical and cytoplasmic flow do not appear to be altered by ANI-1 depletion (Fig. 5A). Consistent with the presence of normal flows, other manifestations of polarity, including the localization of PAR-6:GFP (see Fig. S2 in the supplementary material), asymmetric spindle positioning (Fig. 2D) and nuclear rotation in the P1 cell, and the asynchrony of P1 and AB cell cycle timing (not shown), all occurred normally in *ani-1(RNAi)* embryos (n=12).

To analyze the dynamics of cortical NMY-2, we acquired timelapse sequences of control and ANI-1-depleted embryos expressing NMY-2:GFP. In control embryos, NMY-2:GFP was organized into distinct cortical patches that moved towards and concentrated in the embryo anterior (Fig. 5B, top right) (Munro et al., 2004). By contrast, in *ani-1(RNAi)* embryos, NMY-2:GFP was homogeneously distributed at the cortex. Although it failed to organize into patches, cortical NMY-2:GFP formed a diffuse anterior cap as polarity was established in *ani-1(RNAi)* embryos. We observed similar homogeneous cortical staining and anterior enrichment of endogenous NMY-2 in fixed *ani-1(RNAi)* embryos (data not shown). Kymographs revealed that the small discontinuities of NMY-2:GFP fluorescence visible in ANI-depleted embryos moved towards the anterior (Fig. 5B, bottom right). We conclude that although

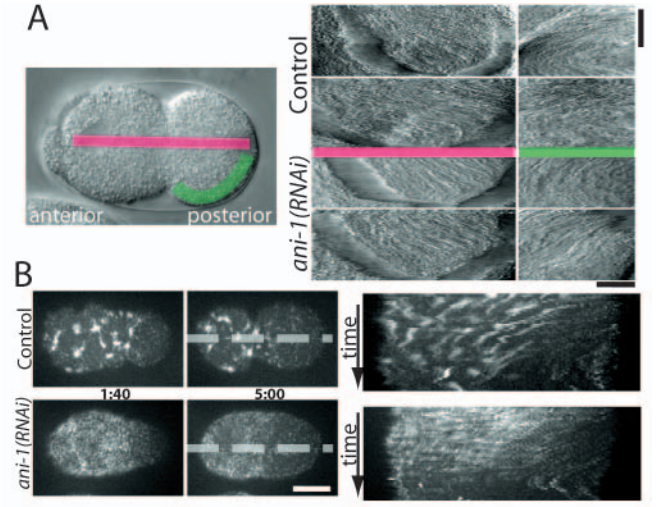

Fig. 5. ANI-1 depletion does not inhibit cortical or cytoplasmic flows or the establishment of polarity. (A) Kymographs of yolk granule flow generated from timelapse DIC sequences of control and *ani-1(RNAi)* embryos collected between meiosis II and pronuclear meeting. Red line: cytoplasmic yolk granules in the center of the embryo flow towards the posterior. Green line: cortical yolk granules in the posterior flow towards the anterior. Vertical scale bar represents 5 minutes; horizontal scale bar represents 10 μm. (B) Left: selected images from timelapse sequences of control and *ani-1(RNAi)* embryos expressing NMY-2:GFP (see also Movies 4 and 5 in the supplementary material). Right: kymographs showing the behavior of cortical NMY-2:GFP over time (8 minutes, 20 seconds preceding pronuclear meeting). The maximum fluorescence intensity for each point across a 2 μm wide box (broken lines) is displayed as a strip (*x*-axis) for each timepoint and placed sequentially to generate kymographs (time is on the *y*-axis). NMY-2:GFP patches (control) and smaller fluorescence discontinuities [*ani-1(RNAi)*] in the embryo posterior moved towards the anterior. Times are given in minutes:seconds. Scale bar: 10 μm.

its organization is disrupted, NMY-2 localizes to the cortex and flows to the anterior in ANI-1-depleted embryos. These results also suggest that organization of NMY-2 into patches and the resulting plasma membrane ingressions are not required for movement of cortical myosin to the anterior, or to generate polarity (see Fig. 9).

ANI-1 is required in somatic tissues

Cytokinesis was not obviously defective in ANI-1-depleted embryos; however, polar body extrusion failed. The aneuploidy resulting from the polar body defect could explain the penetrant embryonic lethality of *ani-1(RNAi)* embryos. To bypass the polar body extrusion defect and examine whether ANI-1 has other essential functions during development, we used *rde-1* mutant worms, which are deficient for RNAi (Tabara et al., 1999). dsRNA directed against *ani-1* was injected into the gonad of *rde-1* mutant mothers that had been mated with wild-type males. Embryos laid between 6 and 10 hours after injection, containing the most dsRNA and a wild-type copy of the *rde-1* gene from the sperm nucleus, were collected. Zygotic transcription of *rde-1* later in embryogenesis initiates RNAi against the target, *ani-1*, after polar body extrusion is completed. ANI-1 depleted progeny produced in this way were viable but displayed a spectrum of developmental defects, including malformed cuticles, uncoordinated movement, protruding vulvae and extruded gonads (see Fig. S3). However, the gonads were well-formed and the depleted worms were not sterile. Males exhibited morphological defects in tail structure. Based on these experiments, we conclude that ANI-1 has crucial functions throughout development.

ANI-2 localizes to the surface of the rachis in the adult gonad

ANI-2 contributes to embryonic viability but was not, somewhat paradoxically, detected in embryos by immunofluorescence or western blotting (Fig. 1E,F). ANI-2-depleted embryos also did not exhibit contractile defects detectable by DIC microscopy (see Fig. S4 and Movie 3 in the supplementary material). One possible explanation for these observations is that ANI-2 functions in the gonad to facilitate the formation of oocytes capable of developing into viable embryos. To test this idea, we examined the localization of ANI-2, NMY-2 and DNA in fixed gonads (Fig. 6). The *C. elegans* hermaphrodite gonad is a syncytium (see schematic in Fig. 6A). Mitotic divisions occur near the distal tip, but the majority of the gonad is lined with nuclei progressing through meiotic prophase in a common cytoplasmic environment. The meiotic nuclei are closely apposed to the gonad surface. Partitions extending from the surface compartmentalize each nucleus in a membrane-bound chamber, or pseudo-cell. Round 'windows' connect each pseudo-cell to the rachis, the central cytoplasmic core of the gonad (Fig. 6A, arrows). At the turn of the gonad, the pseudo-cells increase dramatically in size. Full-sized oocytes populate the proximal gonad, and are fertilized as they pass through the spermatheca.

In control gonads, ANI-2 localized strikingly and exclusively to the surface of the rachis (Fig. 6; green in schematics). ANI-2 framed the windows between the pseudo-cells and the rachis in the distal and middle gonad, and also localized to the surface of the rachis between the windows (Fig. 6A,B). At the turn of the gonad, where developing oocytes increase in size, the 'windows' to the rachis enlarge (Fig. 6A, arrows; Fig. 6C). In the proximal gonad, the ANI-2-stained rachis gradually decreases in diameter, and runs alongside some of the full-sized oocytes in the oviduct. All but approximately the four oocytes that are nearest to the spermatheca appear to be connected to the rachis (Fig. 6A, arrows).

Other cortical cytoskeletal proteins, NMY-2 (Fig. 6), the septin UNC-59 (see Fig. S5 in the supplementary material) and ANI-1 (data not shown), also localized to cortical surfaces in the gonad, but their distributions were distinct from that of ANI-2. The other cortical markers were less specific for the rachis surface and also localized prominently to the lateral surfaces of the developing oocytes. ANI-2 is one of the few proteins known to specifically demarcate the boundaries of the rachis (Vogel and Hedgecock, 2001; Thompson et al., 2002), a localization consistent with its playing an important role in oogenesis and embryo production.

ANI-2 is required for the structural organization of the gonad

To determine how ANI-2 contributes to gonad structure and function, we analyzed *ani-2(RNAi)* worms. Gonads from ANI-

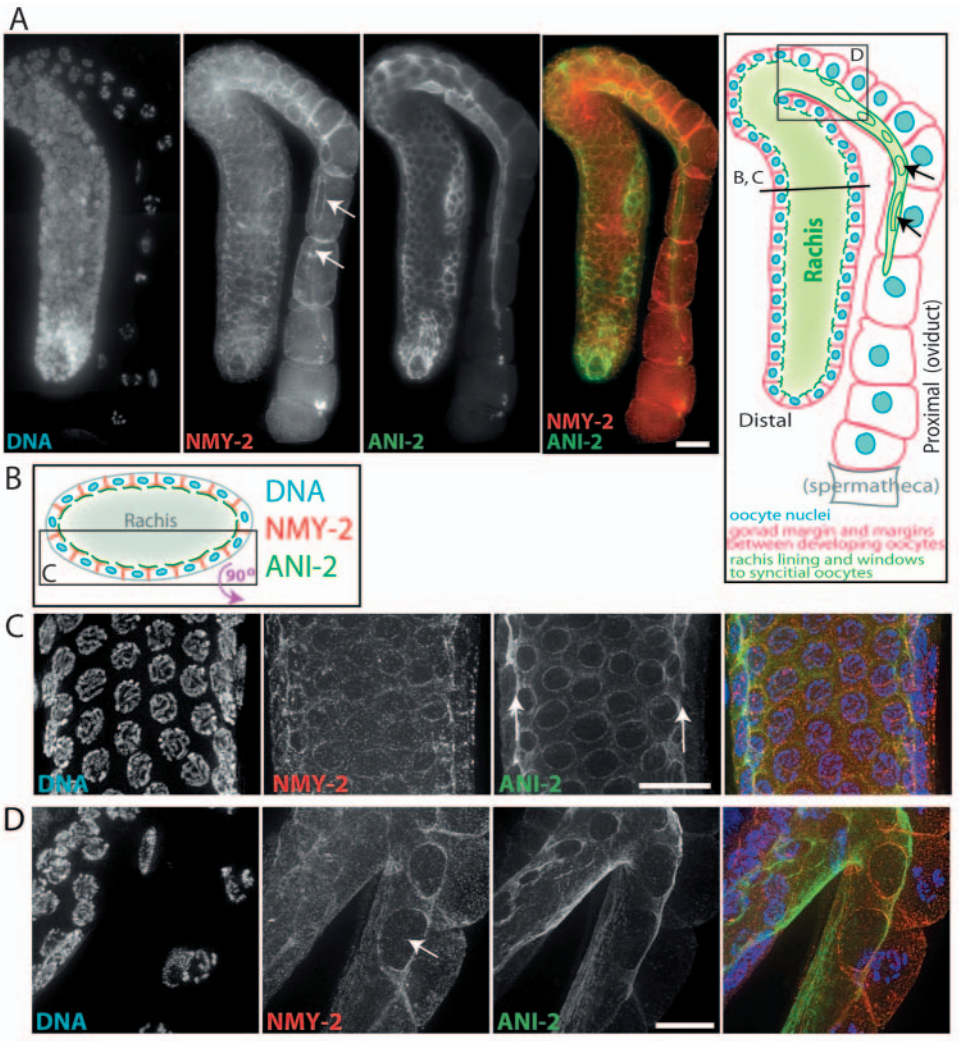

Fig. 6. ANI-2 localizes to the lining of the rachis of the syncytial gonad. Wild-type *C. elegans* syncytial gonads were fixed and stained for DNA, NMY-2 and ANI-2. Images were collected every 0.4 μm through the volume of the gonad. (A) Images of the bottom half of the gonad were projected to visualize the inside surface of the rachis and the openings to the developing oocytes (arrows in A,D). Right: schematic view of the central section of a *C. elegans* gonad. (B) Schematic of a cross-sectional view of the rachis comparing the localization of NMY-2 and ANI-2. Inset box shows region and orientation of view in C. (C) Higher magnification view of the pachytene region of the gonad. Nuclei are regularly spaced. The ANI-2 staining on the surface of the rachis is visible along the edges in cross-section (arrows). (D) Higher magnification view of the bend in the gonad where oocytes increase dramatically in size. The images in C and D are taken from a different gonad from the one shown in A. Scale bars: 10 μm.

2 depleted worms were grossly disorganized. The region of the gonad that ordinarily contains regularly spaced nuclei (Fig. 6) was dramatically shortened: nuclei were randomly positioned and commonly filled the rachis in *ani-2(RNAi)* worms (Fig. 7C). At the bend in the gonad, where oocytes should be midsized and continuous with the rachis, they instead appeared small and tightly packed, eliminating the rachis (Fig. 7A,B, arrowheads). Oocytes in the oviduct were smaller and more variable in size than in control gonads (Fig. 7A,B, arrows). Staining of the septin UNC-59 (see Fig. S5 in the supplementary material) and NMY-2 (Fig. 7) suggested that the partitions between nuclei were either fragmented and disordered or absent in *ani-2(RNAi)* gonads (compare Fig. 6C with Fig. 7C). Both NMY-2 (Fig. 7) and UNC-59 (see Fig. S5 in the supplementary material) still localized to the remaining partitions between developing oocytes, suggesting that their cortical localization does not require ANI-2. However, targeting dependencies are difficult to assess because of the disorganization of the residual structures. Interestingly, in the gonads of *unc-61(e228)* worms in which septins fail to localize to cortical structures (Nguyen et al., 2000), ANI-2 targeted normally to the rachis surface (see Fig. S5 in the supplementary material). Thus, consistent with its localization, ANI-2 plays an important role in gonad structure and oocyte formation.

Oocytes disconnect from the rachis prematurely in ANI-2 depleted worms

In *ani-2(RNAi)* gonads (e.g. Fig. 7B), the oocytes in the oviduct appeared smaller than in controls, suggesting that the rachis is unable to deliver cytoplasm to the developing oocytes to increase their size. To test whether oocytes separate prematurely from the rachis, we developed a method to analyze diffusional continuity between the rachis and oocytes in living worms. We injected rhodamine-labeled dextran into the rachis, allowed it to diffuse within the syncytium and imaged the worms using DIC to visualize structural features of the gonad, as well as fluorescence. In control worms, the dextran diffused throughout the rachis and was detected in all of the developing oocytes except the four or five nearest to the spermatheca (Fig. 8A, 4.8±1.3 oocytes per worm, n=12). By contrast, in worms depleted of ANI-2 ~13 oocytes proximal to the spermatheca did not contain dextran (Fig. 8A, 13.4±4.2 oocytes per worm, n=13). The rachis in the depleted worms also appeared smaller and did not extend around the bend in the gonad.

It seemed likely that the small oocytes in the *ani-2(RNAi)* worms would generate small embryos following fertilization. Indeed, embryos from *ani-2(RNAi)* worms were significantly smaller (average length 40±8.0 μm; n=85) than controls (average length 50±2.6 μm; n=85; Fig. 8B,C). In addition, embryos from ANI-2-depleted worms were highly variable in size (Fig. 8B,C). Depletion of ANI-1 or ANI-3 did not affect embryo size and the effects of ANI-2 depletion were not exacerbated by simultaneous depletion of ANI-1 or ANI-3 (data not shown), indicating that these other anillin family

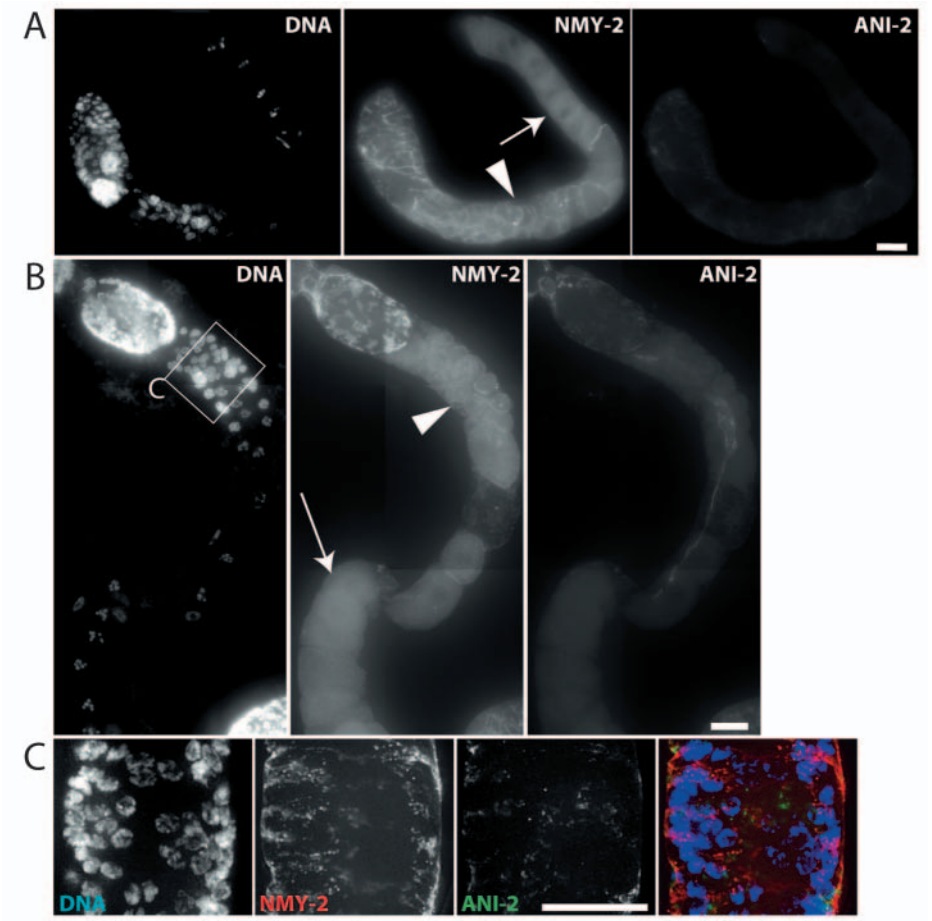

Fig. 7. Depletion of ANI-2 disrupts gonad architecture (compare with wild type in Fig. 6). (A,B) Gonads from worms depleted of ANI-2 by soaking RNAi were extruded, fixed, stained and imaged as for Fig. 6. Scale bars: 10 µm. (C) Higher magnification view representing the indicated region of the gonad in B. Images of a different gonad from that shown above. Scale bar: 10 µm. Arrows indicate abnormally small oocytes in the oviduct; arrowheads indicate tightly packed developing oocytes in the distal gonad.

proteins do not function redundantly with ANI-2 in the gonad. Preliminary studies, in which individual embryos were isolated and their viability assessed, indicate that the partial loss of embryo viability following ANI-2 depletion (Fig. 1C) is due to increased lethality of embryos that are smaller or larger than normal (data not shown). Interestingly, the surviving progeny from ANI-2 depleted worms matured normally and had no adult phenotypes other than significantly reduced brood sizes, demonstrating compromised gonad function [control: 223±16 (s.d.); n=4, *ani-2(RNAi)* progeny: 70±67 (s.d.); n=21, P=0.00018; two-tailed t-test]. Cumulatively, these results suggest that ANI-2 functions specifically in the gonad to maintain the structure of the rachis.

Discussion

Here, we demonstrate distinct localizations and functions for two *C. elegans* anillin homologs. We show that ANI-1 and ANI-2 both contribute to embryonic viability, but via very different mechanisms. ANI-2 is present in the hermaphrodite gonad, where it is required to maintain gonad structure and generate oocytes of uniform size. By contrast, ANI-1 is required for cortical contractile events after oocyte fertilization, including polar body formation and ruffling. We did not uncover a function for ANI-3, as depletion of ANI-3 did not lead to any obvious defects, nor did it enhance defects resulting from depletion of ANI-1 or ANI-2. Additional studies are needed to determine whether ANI-3 has non-essential functions similar to those of ANI-1 or ANI-2, or a unique role not detected by the assays used here.

Functional interactions between anillin family proteins and septins

In vivo and in vitro studies of vertebrate anillins suggest that the PH domain, together with a small adjacent portion of the AH domain, interacts with the septins (Kinoshita et al., 2002; Oegema et al., 2000). The existence of a physical interaction suggests that anillins and septins influence each other's localization or stability. We show that ANI-1 is required for enrichment of the septins in contractile rings during both meiosis and mitosis, whereas the septins are not required to target ANI-1 to contractile rings. A role for anillin in septin recruitment is consistent with analysis of anillin mutants in *Drosophila,* where the phenotypic severity of maternal effect mutations correlates with the degree of disruption of septin recruitment to contractile structures (Field et al., 2005). In *S. pombe,* the anillin related protein Mid2 is not required to recruit septins to the medial ring but does affect the rate at which they turn over (Berlin et al., 2003; Tasto et al., 2003). Like ANI-1, ANI-2 also has C-terminal AH and PH domains but the relationship between ANI-2 and the septins is less clear. ANI-2 localizes to the rachis surface in *unc-61(e228)* septin mutant worms (see Fig. S5 in the supplementary material), indicating that the septins are not required for ANI-2 targeting. The septins also target to residual cortical structures in the gonads of *ani-2(RNAi)* worms (see Fig. S5 in the supplementary material), but the extent of septin recruitment is difficult to assess because of the severe disruption of gonad structure.

The phenotypes we observed when *ani-1(RNAi)* was initiated later in embryogenesis (bypassing the polar body extrusion defect; see Fig. S3 in the supplementary material) are similar to those reported for septin mutant worms (Nguyen et al., 2000). Defects in somatic cytokinesis and cell migration have been reported for septin mutant worms and further studies are necessary to test whether these defects occur in adult *ani-1(RNAi)* animals (Nguyen et al., 2000; Finger et al., 2003). Genetic analyses in *Drosophila* and *S. pombe* provide additional support for a close functional relationship between anillin family proteins and the septins. Mutational inactivation

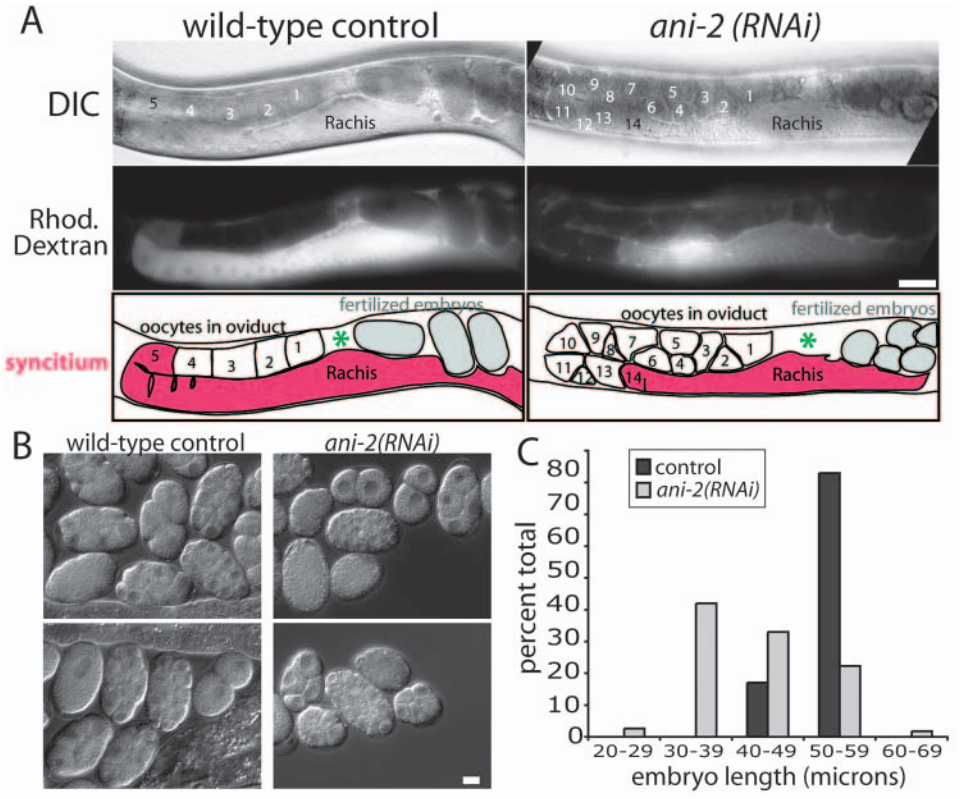

Fig. 8. Oocytes become disconnected from the rachis prematurely in *ani-2(RNAi)* worms. (A) Fluorescent dextran was injected into the gonad rachis of control or *ani-2(RNAi)* worms. Injected worms were imaged by DIC and fluorescence microscopy to visualize the dextran. Schematics summarize results; numbers label oocytes, from the proximal end of the gonad adjacent to the spermatheca (green asterisks). Scale bar: 50 μm. (B) Embryos from control and *ani-2(RNAi)* worms were imaged by DIC microscopy. Scale bar: 10 μm. (C) The lengths of the embryos in B were measured and the distribution plotted for control and *ani-2(RNAi)* worms (n>85 for each condition).

of either results in similar phenotypes in both systems (Adam et al., 2000; Berlin et al., 2003; Neufeld and Rubin, 1994; Tasto et al., 2003; Field et al., 2005).

Although ANI-1 and the septins may function together in many contexts, our results clearly indicate that ANI-1 and ANI-2 have roles independent of the septins in the early embryo and in the gonad. ANI-1 depletion disrupts polar body formation, ruffling and pseudocleavage, and results in penetrant embryonic lethality, whereas septin depletion does not. ANI-2 is required for gonad structure and production of normal oocytes whereas septin mutants do not exhibit gonad defects of similar severity (Nguyen et al., 2000).

A conserved role for anillin family proteins in syncytial structures

Like the early *Drosophila* embryo, the *C. elegans* gonad is a syncytium in which nuclei are cellularized. But unlike the *Drosophila* embryo, where cellularization of all nuclei occurs simultaneously, in the *C. elegans* gonad, meiotic nuclei are cellularized one by one as they move gradually from the distal mitotic zone to the gonad proximal end. In the cellularizing *Drosophila* embryo, anillin promotes the ingression of membrane furrows to create new cell surface between adjacent nuclei and is also required for structural integrity of the newly established partitions (Field et al., 2005). The finding that ANI-2 is important for structural organization of the *C. elegans* gonad during oogenesis highlights a conserved role for anillin family proteins in syncytial structures.

ANI-1 organizes the cortical cytoskeleton to form an inhomogeneous contractile network prior to mitosis

One striking aspect of the ANI-1 depletion phenotype is the complete inhibition of cortical ruffling and pseudocleavage during interphase/prophase. During this cell cycle phase, anillins in other metazoans are sequestered in the nucleus. By contrast, ANI-1 is not detected in the nucleus, has no predicted nuclear localization sequences (the same is true for ANI-2),

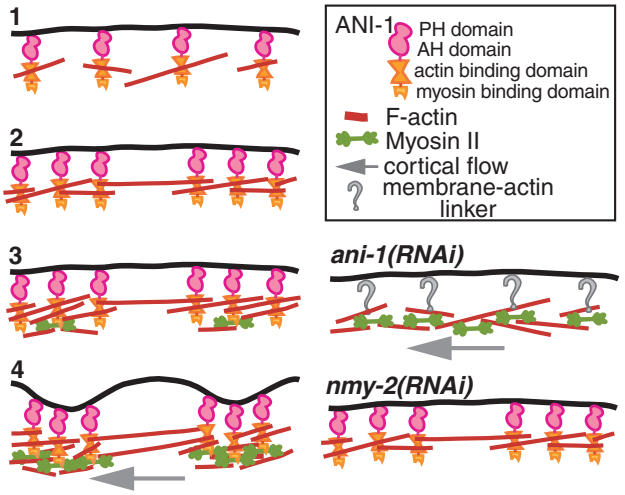

Fig. 9. Model for the role of ANI-1 in the formation of cortical patches. (1) ANI-1 at the plasma membrane binds F-actin. (2) F-actin bound to ANI-1 recruits additional ANI-1 to form a cortical meshwork. (3) Patches of ANI-1 and F-actin recruit myosin II. (4) Myosin II contractility produces ingressions. *ani-1(RNAi)*: patches of cortical myosin II and ingressions fail to form, but flows are normal. *nmy-2(RNAi)*: ANI-1-containing patches still form, but do not ingress and cortical flows fail.

and is present in patches at the base of ingressing ruffles on the cell cortex, together with septins and myosin II. In ANI-1-depleted embryos, both NMY-2 and the septins appear homogenous at the cortex (Figs 4 and 5). In striking contrast, an inhomogeneous network of patches containing AN1-1 and the septins was still present in NMY-2-depleted embryos (Fig. 4), indicating that neither NMY-2 nor productive contractility is required for cortical patch formation. Cumulatively, these results indicate that ANI-1 has a more important role than NMY-2 in organizing the cortical cytoskeleton. Based on the predicted conservation of its F-actin and myosin II-binding domains, we propose a model for the role of ANI-1 in patch formation (Fig. 9). In this model, cortical ANI-1 binds F-actin and bound F-actin recruits additional ANI-1. These two steps might constitute a positive feedback loop that clusters ANI-1, F-actin and the septins to form an inhomogeneous network of cortical patches. NMY-2 also concentrates in the patches (possibly via binding to ANI-1), and provides the contractile force for cortical ingressions. In *ani-1(RNAi)* embryos, the patches fail to form and ruffling does not occur.

Recent studies have suggested that contraction of a dynamic network of acto-myosin containing patches contributes to the establishment of embryonic polarity (Cheeks et al., 2004; Munro et al., 2004). Our results indicate that polarity is successfully established in ANI-1-depleted embryos, despite the failure to form an inhomogeneous network of NMY-2-containing patches or productive cortical ingressions. The essential role of NMY-2 in the establishment of polarity (Guo and Kemphues, 1996) must therefore be independent of its activity and overt clustering to cause cortical ingressions. The ANI-1 phenotype is very similar to that described for *nop-1* mutant embryos, in which polarity is established despite dramatic inhibition of early cortical contractility (Rose et al., 1995). Once the *nop-1* gene has been cloned, it will be interesting to test if it functions in conjunction with ANI-1 to promote cortical ruffling.

Role of anillin family proteins in contractile ring structure and function

Consistent with the failure of cytokinesis completion following anillin disruption in other metazoans, polar body formation is abnormal or fails in ANI-1-depleted *C. elegans* embryos. As myosin II-containing rings form at the site of meiotic cytokinesis in the depleted embryos, it is not known whether this failure results from defects in contractile ring ingression or completion. Determining this will require live imaging of polar body formation, which has so far proven difficult because of their small size and mobility on the embryo surface and the fragility of the embryo egg shell at this stage.

Surprisingly, cytokinesis appears normal in *ani-1(RNAi)* embryos. Although we cannot rule out the possibility that a small amount of residual ANI-1 is sufficient for successful cytokinesis, we think this is unlikely. Quantitative western blotting revealed that ANI-1 is reduced to ~3% of wild-type levels and little or no residual ANI-1 was detected on contractile structures by immunofluorescence. The robust effects of ANI-1 depletion on polar body formation and cortical ruffling also argue against the success of cytokinesis being a consequence of residual ANI-1.

In other systems, anillins are dispensable for the majority of furrow ingression (Echard et al., 2004; Somma et al., 2002; Straight et al., 2005). Thus, one possible explanation for our observation of successful cytokinesis following ANI-1 depletion is the dramatically different geometry of cleavage in *C. elegans* embryos. When *Drosophila* and human cultured cells undergo cytokinesis, they become dumbbell shaped, and an extended bridge is the only connection between the incipient daughter cells. By contrast, in *C. elegans* embryos a new cell-cell boundary forms as the cleavage furrow ingresses. The extensive contacts between the daughter cells may stabilize the small intracellular bridge sufficiently to allow completion of cytokinesis even in the absence of cortical organizing/stabilizing proteins such as anillin.

Given the essential role for ANI-1 in organizing cortical contractility during ruffling and meiotic cytokinesis, why does the mitotic contractile ring form and ingress normally in *ani-1(RNAi)* embryos? Our results suggest two possibilities: (1) an unrelated protein substitutes for ANI-1 in organizing the contractile ring; or (2) the role of ANI-1 in contractile ring function is compensated for by a redundant organizing activity that acts specifically during mitotic cytokinesis. The conservation of anillins and their role in targeting the septins to the contractile ring (Field et al., 2005) lead us to favor the second possibility, but further work is necessary to determine if this is indeed the case.

We thank the members of the Oegema and Desai laboratories, especially Paul Maddox, for their support throughout this project. Joost Monen assisted with imaging fixed gonads. Amy Pasquinelli (UCSD) provided *rde-1* mutant worms. Ed Munro and Jeremy Nance generously provided the strains JJ1479 and JJ1473. We are grateful to Christine Field, Julie Canman, Iain Cheeseman, Alex Dammermann, Defne Yarar and Beth Weaver for helpful discussion and critical readings of this manuscript, and to Jennifer Hsien for assistance. Yuji Kohara (National Institute of Genetics, Mishima, Japan) provided gene-specific cDNAs. CB228 was provided by the Caenorhabditis Genetics Center, which is funded by the NIH National Center for Research Resources (NCRR). This work is supported by funding from the Ludwig Institute for Cancer Research to K.O. and A.D. A.S.M. is a fellow of the Giannini Family Foundation. A.D. is a Damon Runyon Scholar supported by the Damon Runyon Cancer Research Foundation (DRS 38-04). K.O. is a Pew Scholar in the Biomedical Sciences.

Supplementary material

Supplementary material for this article is available at
http://dev.biologists.org/cgi/content/full/132/12/2837/DC1

References

Adam, J. C., Pringle, J. R. and Peifer, M. (2000). Evidence for functional differentiation among *Drosophila* septins in cytokinesis and cellularization. *Mol. Cell. Biol.* **11**, 3123-3135.

Bahler, J., Steever, A. B., Wheatley, S., Wang, Y., Pringle, J. R., Gould, K. L. and McCollum, D. (1998). Role of polo kinase and Mid1p in determining the site of cell division in fission yeast. *J. Cell Biol.* **143**, 1603-1616.

Berlin, A., Paoletti, A. and Chang, F. (2003). Mid2p stabilizes septin rings during cytokinesis in fission yeast. *J. Cell Biol.* **160**, 1083-1092.

Cheeks, R. J., Canman, J. C., Gabriel, W. N., Meyer, N., Strome, S. and Goldstein, B. (2004). *C. elegans* PAR proteins function by mobilizing and stabilizing asymmetrically localized protein complexes. *Curr. Biol.* **14**, 851-862.

Cheeseman, I. M., Niessen, S., Anderson, S., Hyndman, F., Yates, J. R., 3rd, Oegema, K. and Desai, A. (2004). A conserved protein network controls assembly of the outer kinetochore and its ability to sustain tension. *Genes Dev.* **18**, 2255-2268.

Cowan, C. R. and Hyman, A. A. (2004). Asymmetric cell division in *C. elegans*: cortical polarity and spindle positioning. *Annu. Rev. Cell Dev. Biol.* **20**, 427-453.

Desai, A., Rybina, S., Muller-Reichert, T., Shevchenko, A., Hyman, A. and Oegema, K. (2003). KNL-1 directs assembly of the microtubule-binding interface of the kinetochore in *C. elegans*. *Genes Dev.* **7**, 2421-2435.

Echard, A., Hickson, G. R., Foley, E. and O'Farrell, P. H. (2004). Terminal cytokinesis events uncovered after an RNAi screen. *Curr. Biol.* **14**, 1685-1693.

Eggert, U. S., Kiger, A. A., Richter, C., Perlman, Z. E., Perrimon, N., Mitchison, T. J. and Field, C. M. (2004). Parallel chemical genetic and genome-wide RNAi screens identity cytokinesis inhibitors and targets. *Public Library of Science* **2**, 0001-0009.

Field, C. M. and Alberts, B. M. (1995). Anillin, a contractile ring protein that cycles from the nucleus to the cell cortex. *J. Cell Biol.* **131**, 165-178.

Field, C. M., Coughlin, M., Doberstein, S., Marty, T. and Sullivan, W. (2005). Characterization of *anillin* mutants reveals essential roles in septin localization and plasma membrane integrity. *Development* **132**, 2849-2860.

Finger, F. P., Kopish, K. R. and White, J. G. (2003). A role for septins in cellular and axonal migration in *C. elegans*. *Dev. Biol.* **261**, 220-234.

Gonczy, P., Schnabel, H., Kaletta, T., Amores, A. D., Hyman, T. and Schnabel, R. (1999). Dissection of cell division processes in the one cell stage *Caenorhabditis elegans* embryo by mutational analysis. *J. Cell Biol.* **144**, 927-946.

Gonczy, P., Echeverri, C., Oegema, K., Coulson, A., Jones, S. J., Copley, R. R., Duperon, J., Oegema, J., Brehm, M., Cassin, E. et al. (2000). Functional genomic analysis of cell division in *C. elegan*s using RNAi of genes on chromosome III. *Nature* **408**, 331-336.

Guo, S. and Kemphues, K. J. (1996). A non-muscle myosin required for embryonic polarity in *Caenorhabditis elegans*. *Nature* **382**, 455-458.

Hannak, E., Kirkham, M., Hyman, A. A. and Oegema, K. (2001). Aurora-A kinase is required for centrosome maturation in *Caenorhabditis elegans*. *J. Cell Biol.* **155**, 1109-1116.

Hubbard, E. J. and Greenstein, D. (2000). The *Caenorhabditis elegans* gonad: a test tube for cell and developmental biology. *Dev. Dyn.* **218**, 2-22.

Kamath, R. S., Fraser, A. G., Dong, Y., Poulin, G., Durbin, R., Gotta, M., Kanapin, A., Le Bot, N., Moreno, S., Sohrmann, M. et al. (2003). Systematic functional analysis of the *Caenorhabditis elegans* genome using RNAi. *Nature* **421**, 231-237.

Kiger, A. A., Baum, B., Jones, S., Jones, M. R., Coulson, A., Echeverri, C. and Perrimon, N. (2003). A functional genomic analysis of cell morphology using RNA interference. *J. Biol.* **2**, 27.

Kinoshita, M. (2003). The septins. *Genome Biol.* **4**, 236.1-236.9.

Kinoshita, M., Field, C. M., Coughlin, M. L., Straight, A. F. and Mitchison, T. J. (2002). Self- and actin-templated assembly of mammalian septins. *Dev. Cell* **3**, 791-802.

Longtine, M. S., DeMarini, D. J., Valencik, M. L., Al-Awar, O. S., Fares, H., De, Virgilio, C. and Pringle, J. R. (1996). The septins: roles in cytokinesis and other processes. *Curr. Opin. Cell Biol.* **8**, 106-119.

Maeda, I., Kohara, Y., Yamamoto, M. and Sugimoto, A. (2001). Large-scale analysis of gene function in *Caenorhabditis elegans* by high-throughput RNAi. *Curr. Biol.* **11**, 171-176.

Mazumdar, A. and Mazumdar, M. (2002). How one becomes many: blastoderm cellularization in *Drosophila melanogaster*. *BioEssays* **24**, 1012-1022.

Miller, K. G. and Kiehart, D. P. (1995). Fly division. *J. Cell Biol.* **131**, 1-5.

Munro, E., Nance, J. and Priess, J. R. (2004). Cortical flows powered by asymmetrical contraction transport PAR proteins to establish and maintain anterior-posterior polarity in the early *C. elegans* embryo. *Dev. Cell* **7**, 413-424.

Nance, J., Munro, E. M. and Priess, J. R. (2003). C. elegans PAR-3 and PAR-6 are required for abicobasal asymmetries associated with cell adhesion and gastrulation. *Development* **130**, 5339-5350.

Neufeld, T. P. and Rubin, G. M. (1994). The *Drosophila* peanut gene is required for cytokinesis and encodes a protein similar to yeast putative bud neck filament proteins. *Cell* **77**, 371-379.

Nguyen, T. Q., Sawa, H., Okano, H. and White, J. G. (2000). The *C. elegans* septin genes, *unc-59* and *unc-61*, are required for normal postembryonic cytokineses and morphogenesis but have no essential function in embryogenesis. *J. Cell Sci.* **113**, 3825-3837.

Oegema, K., Savoian, M. S., Mitchison, T. J. and Field, C. M. (2000). Functional analysis of a human homologue of the *Drosophila* actin binding protein anillin suggests a role in cytokinesis. *J. Cell Biol.* **150**, 539-552.

Oegema, K., Desai, A., Rybina, S., Kirkham, M. and Hyman, A. A. (2001). Functional analysis of kinetochore assembly in *Caenorhabditis elegans*. *J. Cell Biol.* **153**, 1209-1226.

Piano, F., Schetter, A. J., Mangone, M., Stein, L. and Kemphues, K. J. (2000). RNAi analysis of genes expressed in the ovary of *Caenorhabditis elegans*. *Curr. Biol.* **10**, 1619-1622.

Rogers, S. L., Wiedemann, U., Stuurman, N. and Vale, R. D. (2003). Molecular requirements for actin-based lamella formation in *Drosophila* S2 cells. *J. Cell Biol.* **162**, 1079-1088.

Rose, L. S., Lamb, M. L., Hird, S. N. and Kemphues, K. J. (1995). Pseudocleavage is dispensable for polarity and development in *C. elegans* embryos. *Dev. Biol.* **168**, 479-489.

Simmer, F., Moorman, C., Van Der Linden, A. M., Kuijk, E., Van Den Berghe, P. V., Kamath, R., Fraser, A. G., Ahringer, J. and Plasterk, R. H. (2003). Genome-wide RNAi of *C. elegans* using the hypersensitive *rrf-3* strain reveals novel gene functions. *PLoS Biol.* **1**, E12.

Sohrmann, M., Fankhauser, C., Brodbeck, C. and Simanis, V. (1996). The *dmf1/mid1* gene is essential for correct positioning of the division septum in fission yeast. *Genes Dev.* **10**, 2707-2719.

Somma, M. P., Fasulo, B., Cenci, G., Cundari, E. and Gatti, M. (2002). Molecular dissection of cytokinesis by RNA interference in *Drosophila* cultured cells. *Mol. Biol. Cell* **13**, 2448-2460.

Straight, A. F., Field, C. M. and Mitchison, T. J. (2005). Anillin binds nonmuscle myosin II and regulates the contractile ring. *Mol. Biol. Cell* **16**, 193-201.

Tabara, H., Sarkissian, M., Kelly, W. G., Fleenor, J., Grishok, A., Timmons, L., Fire, A. and Mello, C. C. (1999). The *rde-1* gene, RNA interference, and transposon silencing in *C. elegans. Cell* **99**, 123-132.

Tasto, J. J., Morrell, J. L. and Gould, K. L. (2003). An anillin homologue, Mid2p, acts during fission yeast cytokinesis to organize the septin ring and promote cell separation. *J. Cell Biol.* **160**, 1093-1103.

Thompson, H. M., Skop, A. R., Euteneuer, U., Meyer, B. J. and McNiven, M. A. (2002). The large GTPase dynamin associates with the spindle midzone and is required for cytokinesis. *Curr. Biol.* **12**, 2111-2117.

Vogel, B. E. and Hedgecock, E. M. (2001). Hemicentin, a conserved extracellular member of the immunoglobulin superfamily, organizes epithelial and other cell attachments into oriented line-shaped junctions. *Development* **128**, 883-894.

Wood, W. B. (ed.) (1988). The Nematode Caenorhabditis elegans. Cold Spring Harbor, New York: Cold Spring Harbor Press.

Wu, J. Q., Kuhn, J. R., Kovar, D. R. and Pollard, T. D. (2003). Spatial and temporal pathway for assembly and constriction of the contractile ring in fission yeast cytokinesis. *Dev. Cell* **5**, 723-734.

Table S1. Worm strains used in this study

Strain number	Genotype
N2	Ancestral N2 Bristol strain
CB228	unc-61(e228)V.
JJ1473	unc-119(ed3) III; zuIs45[nmy-2::NMY-2::GFP + unc-119(+)].
JJ1479	unc-119(ed3) III; zuEx77[par-6::PAR-6::GFP + unc-119(+)].
rde-1(ne300)	*rde-1(ne300)*

Table S2. dsRNAs used in this study

Gene number	Name	Oligo 1	Oligo 2	Template
Y49E10.19	*ani-1*	TAATACGACTCACTATAGGTCAAACTCAA TGGAGAGGACAA	AATTAACCCTCACTAAAGGCATTGTGCTT CAAATTCCTCAC	yk488c11
K10B2.5	*ani-2*	TAATACGACTCACTATAGGGAGACCA CCAACGACTCCAAACGTCAGATA	AATTAACCCTCACTAAAGGGTCTCGTCCG TTTCTTGTTTCT	N2 genomic DNA
Y43F8C.14	*ani-3*	TAATACGACTCACTATAGGATTCTGGAGC CCACAAAATG	AATTAACCCTCACTAAAGGGCGGGAAATT CAAAAATTCA	yk208a1
F20G4.3	*nmy-2*	TAATACGACTCACTATAGGAATTGAATCT CGGTTGAAGGAA	AATTAACCCTCACTAAAGGACTGCATTTC ACGCATCTTATG	yk41f5
W09C5.2	*unc-59*	AATTAACCCTCACTAAAGGTCGGACTGCA AATAGCTCGT	TAATACGACTCACTATAGGGCCCATTCGT TTCTTCATTG	yk465c12
Y50E8A.4a	*unc-61*	TAATACGACTCACTATAGGAGCTGTCGAA GCTGGATTTC	AATTAACCCTCACTAAAGGACGGCTGAAC TCGTCTTGAT	yk411f2
Yeast gene	*ndc10*	TAATACGACTCACTATAGGCAAATCGCCC TACACTTCGT	AATTAACCCTCACTAAAGGTCCATTTGGT CCCGTAAAAA	Yeast genomic DNA
Y49E10.19	*ani-1**	AATTAACCCTCACTAAAGGAGCCAAAGG AGACAACTCCA	TAATACGACTCACTATAGGTGCTGATGTA GGTGCAGGAG	N2 cDNA
K10B2.5	*ani-2**	AATTAACCCTCACTAAAGGTTGGATGGGA CTCCAAAAAG	TAATACGACTCACTATAGGCAGCGTGAGG TGTAACGAGA	yk374e5
Y43F8C.14	*ani-3**	AATTAACCCTCACTAAAGGCTTGAAGCCC AAAAATCGAA	TAATACGACTCACTATAGGGCTGAGCCAC GAATTCAAGT	N2 cDNA
Yeast gene	*ctf13*	TAATACGACTCACTATAGGTGTGGAGCTT CCAGGAAAAC	AATTAACCCTCACTAAAGGCTCGATGTTC CACCACTTGA	Yeast genomic DNA

dsRNAs were amplified from either N2 genomic DNA, N2 cDNA or gene-specific cDNAs as indicated.
All dsRNAs were 1-3 mg/ml.
*Second dsRNA used for each anillin protein to ensure specificity.